

Research Article

An NSCT Image Denoising Method Based on Genetic Algorithm to Optimize the Threshold

Zeliang Zhang ¹, Haoyang Wang ¹, Xinwen Bi ¹, Jing Wu ², Yanming Cheng ³,
Ilkyoo Lee ² and Jiufei Chen ⁴

¹College of Computer Science and Technology, Beihua University, China

²Division of Electrical, Electronics & Control Engineering, Kongju National University, Republic of Korea

³College of Electrical and Information Engineering, Beihua University, China

⁴Oil Refinery of Jilin Petrochemical Company, Petro China, China

Correspondence should be addressed to Xinwen Bi; bixinwen@beihua.edu.cn

Received 25 December 2021; Revised 10 April 2022; Accepted 15 April 2022; Published 17 May 2022

Academic Editor: Mukhtaj Khan

Copyright © 2022 Zeliang Zhang et al. This is an open access article distributed under the Creative Commons Attribution License, which permits unrestricted use, distribution, and reproduction in any medium, provided the original work is properly cited.

In order to solve the defect that the threshold value of the NSCT transform method is too large or the real signal coefficients are directly lost during image denoising, an adaptive threshold method of genetic algorithm is used to optimize the NSCT image denoising method. The genetic algorithm is used to generate the initial population, and the genetic operator is determined by selection, crossover, and mutation operations to achieve NSCT threshold optimization. The obtained optimized NSCT threshold is used to process different directions. The coefficients of different scales are processed by using NSCT inverse transform to obtain the denoised image. The results of the case analysis show that the proposed method is used to denoise the image, the peak signal-to-noise ratio of the image after denoising is higher than 30 dB, the image contains rich edge information and detailed information, and the denoising performance is superior.

1. Introduction

Image denoising is an important processing method in the field of image processing. Images are easily contaminated by different noises during acquisition and propagation, which degrade the image quality [1]. Image denoising should preserve the original image details as well as edge information as the key to image process.

The translation invariance of image processing is extremely important to retain image information during image processing [2–5]. The wavelet transform method is usually used to implement the denoising process for images, and the wavelet transform method does not have translation invariance, and the square effect is easily formed when the wavelet transform method is used to process images, and the image edge information is easily lost in the denoising process. Subsampled contourlet transform (SCT) is a transform method with multidirectional, multiresolution, and translation without distortion. The nonsampled contour-

let transform (NSCT) transform method is applied to the image denoising process, and the screening of transform coefficients and the selection of thresholds are the keys to the image denoising performance [6, 7]. The process of estimating the noise variance using the NSCT method is prone to error, resulting in a less precise selection of the threshold.

Liu et al. mainly study the image denoising method based on deep learning algorithm. Through repeated iteration of deep learning algorithm, the threshold value is obtained to make the image clearer [8]; according to Wang Q. et al., based on the optimized variational modal decomposition algorithm, the image is denoised to obtain a clearer image [9]. The above methods can optimize the threshold, but cannot quickly obtain the best threshold. Based on this, this paper proposes an NSCT image denoising method based on genetic algorithm optimization threshold. Genetic algorithm is an efficient optimization algorithm that realizes stochastic optimization by simulating genetic variation in biological evolution and natural selection and does not depend on a

specific solution model with strong global search ability [10, 11]. The process has high threshold optimization efficiency. This paper optimizes the NSCT threshold using a genetic algorithm and uses the optimal NSCT threshold to achieve better image denoising.

In this paper, we propose an NSCT image denoising method based on genetic algorithm optimized threshold, which uses a genetic algorithm to optimize NSCT thresholds and achieves better image denoising using optimal NSCT thresholds.

2. NSCT Image Denoising Method Based on Genetic Algorithm Optimized Threshold

2.1. NSCT Transform. The NSCT transform method achieves image denoising by directional decomposition and scale decomposition of the image, and the overall structure of the NSCT transform is shown in Figure 1.

The NSCT transform first implements a multiscale transform of the image through a non-down sampled tower filter bank and then implements an orientation decomposition of the different scale subband images using a non-down sampled orientation filter [12–14] to obtain subband images with different orientations as well as different scales.

2.1.1. Nonsubsampled Decomposition. The nonsubsampled decomposition of the NSCT transform is achieved by using a multistage iterative approach, and a set of filter formulas that can meet the reconstruction conditions during the non-subsampled decomposition are as follows:

$$L_0(z)G_0(z) + L_1(z)G_1(z) = 1. \quad (1)$$

In Equation (1), $L_0(z)$ and $G_0(z)$ denote the low-pass decomposition filter and high-pass decomposition filter, respectively; $L_1(z)$ and $G_1(z)$ denote the low-pass reconstruction filter and high-pass reconstruction filter, respectively.

The image is divided into high-frequency subbands as well as low-frequency subbands after processing by the filtering of Equation (1), and the repeated iterative filtering of the low-frequency subbands can increase the filter structure.

2.1.2. NSCT Threshold Determination. NSCT uses set thresholds to achieve image denoising, and the selection of thresholds in the NSCT transform is extremely critical. The NSCT transform threshold is usually determined by the Visu shrinkage method with

$$\eta = \delta_n \sqrt{2 * \log N}. \quad (2)$$

In Equation (2), δ_n and N denote the noise standard deviation and the number of coefficients, respectively. When the number of coefficients is large, the threshold value of NSCT transform will be large, and the large threshold value will cause the loss of the true signal coefficients. Based on Equation (2), the adaptive thresholding method is used to determine the NSCT threshold, and the interscale as well as intrascale subband coefficients obtained by the NSCT transform have a high correlation [15]. Based on the decom-

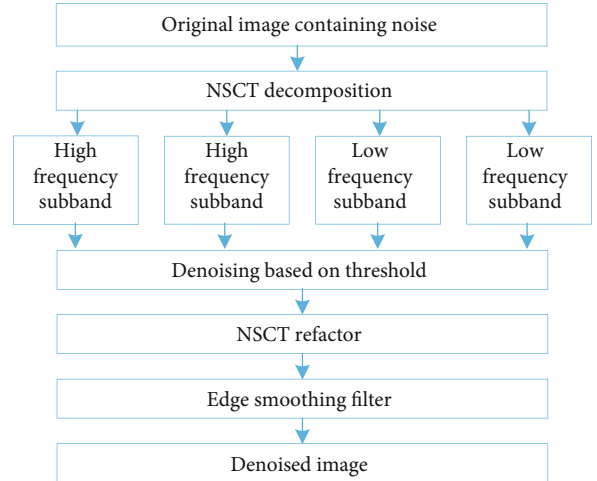


FIGURE 1: Overall structure diagram of NSCT transformation.

position level, the variance of the difference scale noise can be approximated as an exponential distribution, and the noise in different directions is approximately equal within the same scale, and the difference scale noise variance equation can be obtained as

$$\widehat{\delta}_n^2(l) = \widehat{\delta}_n^2(l=1) * e^{1-l^2}. \quad (3)$$

The equation for estimating the minimum scale image noise variance is as

$$\widehat{\delta}_n^2 = \text{Median}(|\omega_{ij}|) / 0.6745. \quad (4)$$

The thresholds are set based on the differential scale noise scenario as

$$T = \delta_n(l) \sqrt{j \times \log(A \times B) / \ln(e + j - 1)}. \quad (5)$$

Equation (5) is a method for acquiring a nonlinear adaptive threshold with decreasing value. The threshold acquired by this method can sharply reduce the noise information as the scale increases. $\delta_n(l)$ and j , respectively, represent the difference scale direction noise standard deviation and the number of directions on the decomposition scale; ω_{ij} and $A \times B$, respectively, represent the wavelet coefficient and image size. The threshold obtained by Equation (5) does not consider intrascale dependence, but only considers interscale dependence. According to the NSCT transformation method, the coefficient energy and noise energy of the image show larger, concentrated, smaller, and dispersed characteristics, respectively, [16, 17]. The target correction Equation (5) is to remove the noise coefficient and retain the image coefficient, and the formula can be obtained as

$$T' = FT. \quad (6)$$

The neighborhood average value is obtained by analyzing the neighborhood of NSCT coefficients, and the

neighborhood window is set to 3×3 . The F can be obtained by comparing the coefficients at this scale as

$$F = \frac{\max(C') \sim C(i, j)}{\max(C) \sim \text{mean}(C)}. \quad (7)$$

In Equation (7), $C(i, j)$ and $\max(C)$, respectively, represent the average value of the neighborhood coefficient after NSCT transformation and the maximum value of the coefficient under the subband, and $\text{mean}(C)$ represents the average value of the coefficient under the subband. Through the analysis and statistics of the NSCT coefficients in the scale, the characteristics of the coefficients in the entire scale and the coefficients in the neighborhood window are compared to obtain the precise positioning of the noise. The absolute value of the coefficient in the noise area and the absolute value of the coefficient in the image information area are the smallest and the largest [18]. For the noise area and the image signal area, increasing the threshold and reducing the threshold can remove more noise and retain more useful information.

2.2. Genetic Algorithm Optimizes NSCT Threshold

2.2.1. Genetic Algorithm. A genetic algorithm is a global search algorithm with high parallelism and effectiveness. The genetic algorithm uses the simulated biological evolution process to search for the optimal solution, uses $P(t)$ to represent the entire operator, and uses the genetic operator to obtain the new group $P(t+1)$. The main operations of the genetic algorithm are as follows:

(1) Choice

According to certain rules and different individual fitness, select good individuals in the t generation group $P(t)$, and inherit them into the next generation group $P(t+1)$.

(2) Cross

For random collocation of individuals in $P(t)$, use a fixed probability to exchange part of the chromosomes between each body.

(3) Variation

Use a fixed probability to convert the gene value at the individual locus in the population $P(t)$ into other alleles.

The flow chart of genetic algorithm optimization is shown in Figure 2.

The genetic algorithm needs to use the symbol string to encode the individual, and select the binary encoding method to encode the individual. Randomly select the starting search point as the initial population data. Determine the strengths and weaknesses of different individuals based on their fitness, and use the acquired fitness to determine genetic opportunities. Inherit individuals with higher fitness in a population to the next population, according to a fixed rule which is a selection operation [19, 20], and a propor-

tional selection method is selected to implement the selection operation of the genetic algorithm. The crossover operation in the genetic algorithm is the process of forming a new individual. The crossover operation exchanges chromosomes between different individuals according to a fixed probability, and the single-point crossover method is selected to implement the genetic algorithm crossover operation. Randomly pair the population, set the position of the intersection, and pair some genes between the chromosomes. Mutation calculation is an operation method to form a new individual, to determine the genetic mutation position of all individuals, and to reverse the original gene value of the mutation point according to a fixed probability.

2.2.2. NSCT Threshold Optimization. Genetic algorithms are optimization methods that use biogenetic concepts to obtain optimal solutions to problems and determine the optimal threshold of NSCT using genetic algorithms.

The fitness function is the core of the genetic algorithm, and the fitness function needs to be determined based on the objective function of the problem to be solved, and the fitness function is used to clarify the advantages and disadvantages of individuals within the population group [21], which is an important basis for the natural selection of the genetic algorithm. The image information entropy after denoising is set as the threshold to optimize the objective function, so that the amount of image information after denoising contains image detail information as well as texture information.

η represents the NSCT threshold, and F_η represents the image after denoising. The available fitness function formula is

$$\text{Fitness}(\eta) = \text{entropy}(F_\eta). \quad (8)$$

The genetic algorithm optimizes the NSCT threshold process as follows:

(1) *Generate an Initial Population.* Real number coding is used as the coding scheme, and real number coding is highly effective for function optimization problems [22]. Generate the initial population, set the adaptive threshold range to [0.5, 0.8], randomly generate a population uniformly distributed in this range, denoted by $\{\eta_1, \eta_2, \dots, \eta_N\}$, and select the optimal η_i to maximize the information entropy of the denoised image.

(2) *Determination of Genetic Operator.* The genetic operator is determined by selection, crossover, and mutation operators. Use the replication process to complete the operator selection, select individuals with higher fitness in the population, and obtain the independent individual probability formula as

$$P(X_i) = \frac{\text{Fit}(X_i)}{\sum_{i=1}^N \text{Fit}(X_i)}. \quad (9)$$

Crossover operations are realized by reorganizing individuals, and crossover operations are the main part of

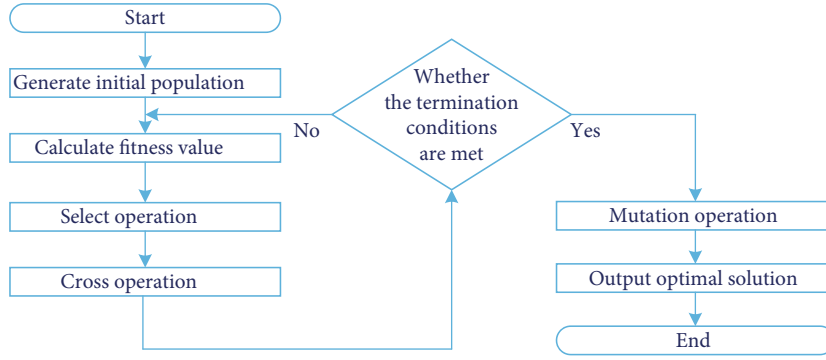


FIGURE 2: Flow chart of genetic algorithm optimization.

forming new individuals. Select the number of pairs of N_s to generate the individual pairs in the form of $[\eta_i, \eta_j]$. The number of individual pairs is $N_s/2$, and the intermediate recombination method is selected to be used in the real-valued encoding process. The operating formula is

$$\eta'_i = \eta_i + \theta_i (\eta_j - \eta_i). \quad (10)$$

In Equation (10), θ represents the conversion factor uniformly generated in the interval.

The mutation operator is used to randomly generate a new value in the range and disturb the original gene value, and the mutation operation formula is as follows:

$$\eta' = \eta + \varphi. \quad (11)$$

In Equation (11), η' and φ , respectively, represent the postmutation threshold and the randomly formed range of variable asynchronous length within $[-1,1]$.

The process of the NSCT image denoising method based on genetic algorithm optimization threshold is as follows:

- (1) Use NSCT transform to process images containing noise
- (2) Obtain the noise variance of images of different scales according to formula (3), and use Equation (5) to set the threshold of each subband
- (3) Use formula (6) to obtain the modified adaptive threshold
- (4) Use genetic algorithm to obtain optimal adaptive threshold
- (5) Use the obtained optimal adaptive threshold to process coefficients in different directions and different scales, and obtain the denoised image through inverse transformation

3. Example Applications

The CoPhIR dataset, a commonly used image processing dataset in the network, is selected as the experimental test

dataset, which contains classical images such as Lena, fruits, horse, and airplane. The weighted variational method and the mathematical morphological filtering method are selected as the comparison methods. The image denoising performance of the method in this paper is verified by both qualitative analysis as well as quantitative analysis.

3.1. Qualitative Analysis. The original standard test image Lena image containing Gaussian white noise in the test dataset is shown in Figure 3.

The final image obtained by using the proposed method in this paper to denoise the image is shown in Figure 4.

The experimental comparison results in Figures 3 and 4 show that the proposed method in this paper can effectively remove the noise contained in the original image and effectively retain the image edge information as well as the detail information, and the image contrast is higher after denoising. This verifies that the method in this paper has a high image denoising effect.

3.2. Quantitative Analysis. The methods in literature [8] and literature [9] are selected as comparison methods to process images together with the method in this paper. The smoothness index, peak signal-to-noise ratio, edge retention index, and image information entropy indexes after denoising are compared to prove the advancement of the method in this paper.

The smoothing index is chosen as the evaluation of the smoothing ability of the method in this paper on noise, and the smoothing index is calculated as

$$FI = U/SV. \quad (12)$$

In Equation (12), SV and U are, respectively, the standard deviation of all pixels and the average value of all pixels in a certain area after image denoising. The higher image-smoothing index, the higher the smoothing effect of the denoising method.

The comparison results of the smoothing index of the denoised images under different decomposition layers are shown in Figure 5.

From the experimental results in Figure 5, it can be seen that with the increase of the number of image decomposition layers, the smoothness index of the image increases. In



FIGURE 3: Original image containing noise.



FIGURE 4: Image after denoising.

the case of different decomposition layers, the smoothness index of the method in this paper is the highest, which is better than the comparison method, which effectively verifies that the method in this paper has high image denoising performance.

The peak signal-to-noise ratio is selected as another indicator to evaluate the effect of image denoising. The formula for calculating the peak signal-to-noise ratio is

$$PSNR = 10 \lg \frac{I_{\max} \times I_{\max}}{1/AB \sum_{i=1}^A \sum_{j=1}^B (I_{i,j} - \hat{I}_{i,j})^2}. \quad (13)$$

In Equation (13), I_{\max} and A, B , respectively, represent the maximum gray value of the image and the number of image rows and columns; $I_{i,j}$ and $\hat{I}_{i,j}$, respectively, represent the gray value of the pixel (i,j) before denoising and the pixel (i,j) after denoising grayscale value.

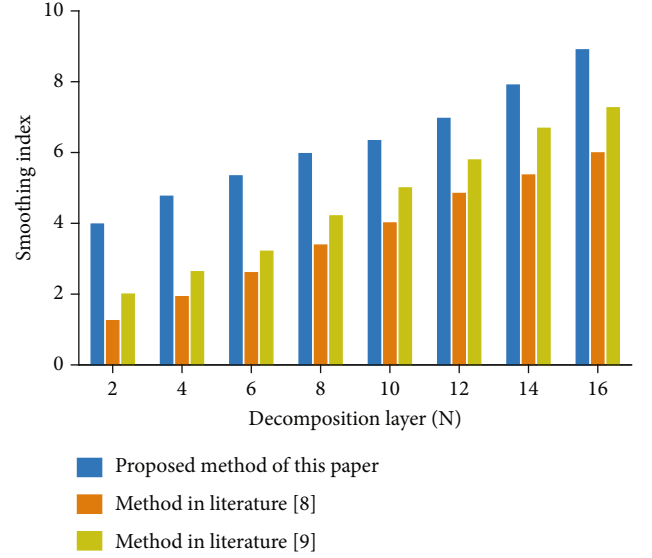


FIGURE 5: Smoothing index comparison.

The comparison results of the peak signal-to-noise ratio of 10 images in the test dataset of different methods are shown in Table 1.

The edge retention index is used to measure the horizontal and vertical edge retention of the original image after denoising. The calculation equation for the horizontal and vertical edge retention index is as follows:

$$EPI_H = \frac{\sum_{i=1}^A \sum_{j=1}^{B-1} |\hat{I}_{i,j+1} - \hat{I}_{i,j}|}{\sum_{i=1}^A \sum_{j=1}^{B-1} |I_{i,j+1} - I_{i,j}|}, \quad (14)$$

$$EPI_V = \frac{\sum_{i=1}^A \sum_{j=1}^{B-1} |\hat{I}_{i+1,j} - \hat{I}_{i,j}|}{\sum_{i=1}^A \sum_{j=1}^{B-1} |I_{i+1,j} - I_{i,j}|}. \quad (15)$$

The smoothing index is chosen as the evaluation of the smoothing ability of the method in this paper on noise, and the smoothing index is calculated in Table 2.

The experimental results in Tables 1 and 2 show that, compared with the methods in [8, 9], the peak signal-to-noise ratio of denoised images is higher than 30 dB, and the horizontal and vertical edge retention indices of denoised images are higher than 1.5, the peak signal-to-noise ratio and image edge index of the denoised test image are both optimal, and the experimental results show that this method has high image denoising performance. The processed images contain rich edge information, indicating that the method has high denoising performance.

The image information entropy can measure the detail information contained in the denoised image, and the higher the image information entropy result, the more detail information is contained in the image, and the better the image denoising performance is. The comparison results of image information entropy obtained by using three methods for image denoising are shown in Table 3.

TABLE 1: Comparison of peak signal-to-noise ratio.

Image number	The original image/dB	The proposed method of this paper	Method of literature [8]/dB	Method of literature [9]/dB
1	13.52	34.52	27.21	29.52
2	16.52	92.75	27.64	21.75
3	14.75	37.52	29.52	28.43
4	16.52	34.52	24.52	27.75
5	17.75	36.75	23.37	24.54
6	16.52	31.52	27.54	24.32
7	13.54	33.23	21.51	26.42
7	15.52	37.75	25.63	27.75
9	13.52	36.52	23.56	27.64
10	14.75	31.45	27.04	28.45

TABLE 2: Comparison of edge retention index.

Image number	The proposed method of this paper		Method of literature [8]/dB		Method of literature [9]/dB	
	EPI _H	EPI _V	EPI _H	EPI _V	EPI _H	EPI _V
1	1.7579	1.6521	0.9752	1.3512	1.0521	0.7621
2	1.5274	1.4975	0.7451	1.2415	1.2154	0.7715
3	1.6325	1.7524	1.2516	1.3254	1.3214	0.9561
4	1.5742	1.5796	1.1577	1.2547	1.2514	0.7521
5	1.6355	1.6254	1.2354	1.1524	1.1752	1.1254
6	1.7422	1.7521	1.3521	0.9754	1.05275	0.0975
7	1.5746	1.6571	1.2745	1.2541	0.9752	1.1072
7	1.4752	1.5741	1.2514	0.9521	0.7542	1.1205
9	1.6125	1.7526	1.1975	1.1754	0.7572	1.2354
10	1.5975	1.5974	0.9452	1.2544	1.1352	1.0751

TABLE 3: Comparison of information entropy.

Image number	The proposed method of this paper	Method of literature [8]/dB	Method of literature [9]/dB
1	7.8541	7.1757	7.0457
2	7.6857	7.2545	7.1423
3	7.5826	7.2334	7.2534
4	7.4571	7.1584	7.4542
5	7.5675	7.3415	7.1021
6	7.7845	7.2514	7.2024
7	7.7154	7.3346	7.0151
8	7.6524	7.2521	7.3152
9	7.5646	7.1635	7.0675
10	7.6752	7.0545	7.1547

The experimental results in Table 3 show that the entropy of different image information obtained by denoising the image with this method is higher than that of the other two methods, which indicates that the denoising of the image with this method can effectively retain the image

detail information and make the denoised image information richer. This method can clearly present the overall information of the image and retain more details, which verifies that this method has high image denoising performance and can meet the demand of image denoising to maximize the detail retention.

4. Conclusion

The genetic algorithm is applied to the NSCT image denoising method, and the genetic algorithm has a high global optimizing performance to implement threshold optimization for the NSCT image denoising method. By obtaining the optimal denoising thresholds for each NSCT image sub-band, image denoising is achieved by processing the decomposed NSCT coefficients with the obtained thresholds. The proposed method can achieve effective optimization of the threshold value of NSCT image denotation method, which can be applied in practical applications of image processing. The example analysis verifies that the proposed method has high image denoising processing performance. Using the method to denoise the image can effectively remove the Gaussian white noise of the image, so that the processed

image has a higher peak signal-to-noise ratio. After denoising, the image retains the edge information and detail information of the original image, gives full play to the displacement invariance property of NSCT, and satisfies the position shift requirements of image denoising, and the edge information is kept intact. This effectively improves the blurring of the image texture and enhances the visual effect of the image.

Data Availability

The data used to support the findings of this study are available from the corresponding author upon request.

Conflicts of Interest

The authors declare that there are no conflicts of interest regarding the publication of this paper.

Acknowledgments

This paper was supported by the Jilin Provincial Department of Education Project: Research on Remote Sensing Image Fusion Enhancement Algorithm Based on Improved NSCT (Grant JJKH20210047KJ), Beihua University Project: Cloud Platform Construction of Shanxi New Era Civilization Practice Center (Grant 202003015), Development Plan Project of Jilin Provincial Science and Technology Department (Grant 20210203050SF), and Jilin Provincial Department of Education Project (Grant JJKH20220056KJ). Also thanks are due to Mingjie Ma and Yingjian Shao for editing this paper.

References

- [1] Z. Zhang, C. Deng, and X. Yue, "A fingerprint image denoising method with improved threshold function," *Journal of Harbin University of Science and Technology*, vol. 27, no. 1, pp. 55–60, 2022.
- [2] J. Xu and Q. Zhang, "Research and application of improved wavelet soft threshold function in image denoising," *Computer Engineering and Science*, vol. 44, no. 1, pp. 92–101, 2022.
- [3] M. Zheng, G. Qi, Z. Zhu, Y. Li, H. Wei, and Y. Liu, "Image dehazing by an artificial image fusion method based on adaptive structure decomposition," *IEEE Sensors Journal*, vol. 20, no. 14, pp. 8062–8072, 2020.
- [4] Z. Zhu, H. Wei, G. Hu, Y. Li, G. Qi, and N. Mazur, "A Novel fast single image dehazing algorithm based on artificial multi-exposure image fusion," *IEEE Transactions on Instrumentation and Measurement*, vol. 70, pp. 1–23, 2021.
- [5] Y. X. Li and L. Wang, "A novel noise reduction technique for underwater acoustic signals based on complete ensemble empirical mode decomposition with adaptive noise, minimum mean square variance criterion and least mean square adaptive filter," *Defence Technology*, vol. 16, no. 3, pp. 543–554, 2020.
- [6] Y. Su, S. Jin, X. Zhang, X. Shen, M. R. Eden, and J. Ren, "Stakeholder-oriented multi-objective process optimization based on an improved genetic algorithm," *Computers & Chemical Engineering*, vol. 132, p. 106618, 2020.
- [7] W. Wang, C. Zhang, and M. K. Ng, "Variational model for simultaneously image denoising and contrast enhancement," *Optics Express*, vol. 28, no. 13, p. 17751, 2020.
- [8] D. Liu, J. Jia, Y. Zhao, and Y. Qian, "A review of image denoising methods based on deep learning," *Computer Engineering and Applications*, vol. 57, no. 7, pp. 1–13, 2021.
- [9] Q. Wang, X. Wang, and B. Wang, "Denoising of echo signals based on optimized variational mode decomposition algorithm," *Progress in Lasers and Optoelectronics*, vol. 57, no. 20, pp. 79–92, 2021.
- [10] Z. Zhu, Y. Luo, G. Qi, J. Meng, Y. Li, and N. Mazur, "Remote sensing image defogging networks based on dual self-attention boost residual octave convolution," *Remote Sensing*, vol. 13, no. 16, p. 3104, 2021.
- [11] Z. Zhu, Y. Luo, H. Wei et al., "Atmospheric light estimation based remote sensing image dehazing," *Remote Sensing*, vol. 13, no. 13, p. 2432, 2021.
- [12] W. Yuan, B. Liu, Z. Wang et al., "Research on insulator hydrophobic image denoising based on guided filtering algorithm," *Journal of Electric Power Science and Technology*, vol. 36, no. 3, pp. 135–140, 2021.
- [13] F. Cao, "Research on image denoising method based on multi-scale analysis," *Software*, vol. 42, no. 7, pp. 7–10, 2021.
- [14] Y. Xu, Y. Qian, and J. Wang, "Image denoising method in contourlet domain with improved Bayesian threshold," *Journal of Xinxiang University*, vol. 37, no. 6, pp. 42–45, 2020.
- [15] Y. Zang, Y. Qian, X. Chen, G. Sheng, and X. Jiang, "Application of photoelectric image fusion method based on non-subsampling contourlet transform in GIL partial discharge detection," *High Voltage Technology*, vol. 47, no. 2, pp. 519–527, 2021.
- [16] M. Guan, J. Zhu, and Y. Wu, "Research progress on image denoising methods. Computer Times," vol. 2, p. 29-32+35, 2020.
- [17] Y. Liu, H. Hui, Y. Lu, X. Zou, Y. Yang, and J. Cao, "Multi-source information fusion indoor positioning method based on genetic algorithm optimization neural network," *Chinese Journal of Inertial Technology*, vol. 27, no. 1, pp. 67–73, 2020.
- [18] Y. Song and L. Zhou, "Multi-band SAR image fusion algorithm based on dual feature quantities and NSCT," *Signal Processing*, vol. 36, no. 1, pp. 93–101, 2020.
- [19] X. Ju and F. Liu, "Wind farm layout optimization using self-informed genetic algorithm with information guided exploitation," *Applied Energy*, vol. 248, pp. 429–445, 2019.
- [20] H. Golshan and R. P. R. Hasanzadeh, "Fuzzy hysteresis smoothing: a new approach for image denoising," *IEEE Transactions on Fuzzy Systems PP*, vol. 99, pp. 1–11, 2019.
- [21] A. Paykani, C. E. Frouzakis, and K. Boulouchos, "Numerical optimization of methane-based fuel blends under engine-relevant conditions using a multi-objective genetic algorithm," *Applied Energy*, vol. 242, pp. 1712–1724, 2019.
- [22] X. Wang, L. Yin, M. Gao, Z. Wang, and G. Zou, "Denoising method for passive photon counting images based on block-matching 3D filter and non-subsampled contourlet transform," *Sensors*, vol. 19, no. 11, p. 2462, 2019.